Deep sequencing in conjunction with expression and functional analyses reveals activation of FGFR1 in ewing sarcoma

Agelopoulos, Konstantin ; Richter, Günther H S ; Schmidt, Eva ; Dirksen, Uta ; von Heyking, Kristina ; Moser, Benjamin ; Klein, Hans-Ulrich ; Kontny, Udo ; Dugas, Martin ; Poos, Kathrin ; Korsching, Eberhard ; Buch, Thorsten ; Weckesser, Matthias ; Schulze, Isabell ; Besoke, Regina ; Witten, Anika ; Stoll, Monika ; Köhler, Gabriele ; Hartmann, Wolfgang ; Wardelmann, Eva ; Rossig, Claudia ; Baumhoer, Daniel ; Jürgens, Heribert ; Burdach, Stefan ; Berdel, Wolfgang E ; Müller-Tidow, Carsten

Abstract: PURPOSE: A low mutation rate seems to be a general feature of pediatric cancers, in particular in oncofusion gene-driven tumors. Genetically, Ewing sarcoma is defined by balanced chromosomal EWS/ETS translocations, which give rise to oncogenic chimeric proteins (EWS-ETS). Other contributing somatic mutations involved in disease development have only been observed at low frequency. EXPERIMENTAL DESIGN: Tumor samples of 116 Ewing sarcoma patients were analyzed here. Whole-genome sequencing was performed on two patients with normal, primary, and relapsed tissue. Whole-exome sequencing was performed on 50 Ewing sarcoma and 22 matched normal tissues. A discovery dataset of 14 of these tumor/normal pairs identified 232 somatic mutations. Recurrent nonsynonymous mutations were validated in the 36 remaining exomes. Transcriptome analysis was performed in a subset of 14 of 50 Ewing sarcomas and DNA copy number gain and expression of FGFR1 in 63 of 116 Ewing sarcomas. RESULTS: Relapsed tumors consistently showed a 2- to 3-fold increased number of mutations. We identified several recurrently mutated genes at low frequency (ANKRD30A, CCDC19, KIAA0319, KIAA1522, LAMB4, SLFN11, STAG2, TP53, UNC80, ZNF98). An oncogenic fibroblast growth factor receptor 1 (FGFR1) mutation (N546K) was detected, and the FGFR1 locus frequently showed copy number gain (31.7%) in primary tumors. Furthermore, high-level FGFR1 expression was noted as a characteristic feature of Ewing sarcoma. RNA interference of FGFR1 expression in Ewing sarcoma lines blocked proliferation and completely suppressed xenograft tumor growth. FGFR1 tyrosine kinase inhibitor (TKI) therapy in a patient with Ewing sarcoma relapse significantly reduced 18-FDG-PET activity. CONCLUSIONS: FGFR1 may constitute a promising target for novel therapeutic approaches in Ewing sarcoma.

DOI: https://doi.org/10.1158/1078-0432.CCR-14-2744

Heribert; Burdach, Stefan; Berdel, Wolfgang E; Müller-Tidow, Carsten (2015). Deep sequencing in conjunction with expression and functional analyses reveals activation of FGFR1 in ewing sarcoma. Clinical Cancer Research, 21(21):4935-4946.
DOI: https://doi.org/10.1158/1078-0432.CCR-14-2744

Published OnlineFirst July 15, 2015; DOI: 10.1158/1078-0432.CCR-14-2744

Biology of Human Tumors

Clinical Cancer Research

Deep Sequencing in Conjunction with Expression and Functional Analyses Reveals Activation of FGFR1 in Ewing Sarcoma

Konstantin Agelopoulos[1], Günther H.S. Richter[2], Eva Schmidt[1], Uta Dirksen[3], Kristina von Heyking[2], Benjamin Moser[1], Hans-Ulrich Klein[4], Udo Kontny[5], Martin Dugas[4], Kathrin Poos[6], Eberhard Korsching[6], Thorsten Buch[7,8], Matthias Weckesser[9], Isabell Schulze[1,10], Regina Besoke[11], Anika Witten[12], Monika Stoll[12], Gabriele Köhler[13], Wolfgang Hartmann[14], Eva Wardelmann[14], Claudia Rossig[3], Daniel Baumhoer[15], Heribert Jürgens[3], Stefan Burdach[2], Wolfgang E. Berdel[1], and Carsten Müller-Tidow[1,10]

Abstract

Purpose: A low mutation rate seems to be a general feature of pediatric cancers, in particular in oncofusion gene-driven tumors. Genetically, Ewing sarcoma is defined by balanced chromosomal *EWS/ETS* translocations, which give rise to oncogenic chimeric proteins (EWS-ETS). Other contributing somatic mutations involved in disease development have only been observed at low frequency.

Experimental Design: Tumor samples of 116 Ewing sarcoma patients were analyzed here. Whole-genome sequencing was performed on two patients with normal, primary, and relapsed tissue. Whole-exome sequencing was performed on 50 Ewing sarcoma and 22 matched normal tissues. A discovery dataset of 14 of these tumor/normal pairs identified 232 somatic mutations. Recurrent nonsynonymous mutations were validated in the 36 remaining exomes. Transcriptome analysis was performed in a subset of 14 of 50 Ewing sarcomas and DNA copy number gain and expression of FGFR1 in 63 of 116 Ewing sarcomas.

Results: Relapsed tumors consistently showed a 2- to 3-fold increased number of mutations. We identified several recurrently mutated genes at low frequency (*ANKRD30A, CCDC19, KIAA0319, KIAA1522, LAMB4, SLFN11, STAG2, TP53, UNC80, ZNF98*). An oncogenic fibroblast growth factor receptor 1 (*FGFR1*) mutation (N546K) was detected, and the *FGFR1* locus frequently showed copy number gain (31.7%) in primary tumors. Furthermore, high-level FGFR1 expression was noted as a characteristic feature of Ewing sarcoma. RNA interference of FGFR1 expression in Ewing sarcoma lines blocked proliferation and completely suppressed xenograft tumor growth. FGFR1 tyrosine kinase inhibitor (TKI) therapy in a patient with Ewing sarcoma relapse significantly reduced 18-FDG-PET activity.

Conclusions: FGFR1 may constitute a promising target for novel therapeutic approaches in Ewing sarcoma. *Clin Cancer Res; 21(21); 4935–46. ©2015 AACR.*

Introduction

Ewing sarcoma is a highly malignant bone and soft tissue neoplasia of still enigmatic histogenesis with a prominent *stemness* phenotype (1, 2). Histogenesis may be endothelial, neuroectodermal (3–5), or osteochondrogenic (6, 7). Genetically, Ewing sarcoma is defined by specific balanced chromosomal *EWS/ETS* translocations that give rise to oncogenic chimeric proteins (EWS-ETS), the most common being EWS-FLI1

[1]Department of Medicine A, Hematology, and Oncology, University Hospital of Muenster, Muenster, Germany. [2]Children's Cancer Research Center and Department of Pediatrics, Klinikum rechts der Isar, Technische Universität München and Comprehensive Cancer Center Munich (CCCM), Munich, Germany, together with the German Cancer Consortium (DKTK), Germany. [3]Department of Pediatric Oncology and Hematology, University Children's Hospital Muenster, Muenster, Germany. [4]Institute of Medical Informatics, University of Muenster, Muenster, Germany. [5]Department of Pediatrics, Medical Faculty, RWTH Aachen University, Aachen, Germany. [6]Institute of Bioinformatics, University Hospital of Muenster, Muenster, Germany. [7]Institute for Medical Microbiology, Immunology and Hygiene, Technische Universität München, Munich, Germany. [8]Institute of Laboratory Animal Science, University of Zurich, Zurich, Switzerland. [9]Department of Nuclear Medicine, University of Muenster, Muenster, Germany. [10]Department of Medicine IV, Hematology and Oncology, State Center for Cell and Gene Therapy, University Hospital Halle, Halle (Saale), Germany. [11]Institute of Human Genetics, University of Muenster, Muenster, Germany. [12]Institute of Human Genetics, Genetic Epidemiology, University of Muenster, Muenster, Germany. [13]Institute of Pathology, Klinikum Fulda, Fulda, Germany. [14]Department of Pathology, University of Muenster, Muenster, Germany. [15]Bone Tumor Reference Center at the Institute of Pathology, University Hospital Basel, Basel, Switzerland.

Note: Supplementary data for this article are available at Clinical Cancer Research Online (http://clincancerres.aacrjournals.org/).

K. Agelopoulos, G.H.S. Richter, and E. Schmidt share first authorship.

W.E. Berdel and C. Müller-Tidow share senior authorship.

Corresponding Authors: Carsten Müller-Tidow, University Hospital Halle, Department of Medicine IV, Hematology and Oncology, Ernst-Grube-Street 40, 06120 Halle (Saale), Germany. Phone: 49-345-557-4972; Fax: 49-345-557-2950; E-mail: carsten.mueller-tidow@uk-halle.de; and Günther H.S. Richter, Technische Universität München, Children's Cancer Research Center and Department of Pediatrics, Koelner Platz 1, 80804 Munich, Germany. Phone: 49-89-3068-3235; Fax: 49-89-3068-3791; E-mail: guenther.richter@lrz.tum.de

doi: 10.1158/1078-0432.CCR-14-2744

Published OnlineFirst July 15, 2015; DOI: 10.1158/1078-0432.CCR-14-2744

Translational Relevance

Pediatric cancers, including Ewing sarcoma, are characterized by a low mutation count with difficult-to-target driver lesions. Our investigation provides evidence that integration of sequencing data with gene amplification, expression, and functional analysis is crucial to identify oncogenic drivers in cancers with low rates of recurrent mutations. By this approach, aberrant FGFR1 activity emerged as a novel target for Ewing sarcoma. FGFR1 inhibitors are in clinical trials for other cancers and could be tested in Ewing sarcoma with different ways of FGFR1 activation.

as a consequence of the t(11;22)(q24;q12) translocation (8–11).

EWS-ETS chimeric proteins promote cell transformation through abnormal regulation of specific target genes involved in the control of a variety of cellular processes (12). However, little is known about cooperating events that affect oncogenesis and/or progression of Ewing sarcoma. *TP53* mutations and *CDKN2A* deletions are known to confer poor prognosis but are infrequently observed for this sarcoma (~13% of cases; ref. 13). Furthermore, despite a relatively stable genome, copy number alterations (CNA) are recurrently observed in Ewing sarcoma (14), but only 1q gains as detected in 31% of tumor samples seem to be associated with poor prognosis (15). In genome-wide association studies (GWAS), few genomic loci were associated with susceptibility (16).

Cancer arises due to genetic mutations that alter the function of a wide array of genes (17). Cancer genomes are often aneuploid, contain amplifications and deletions, and typically comprise hundreds to thousands of DNA point mutations. However, not all cancers are necessarily that complex. Large-scale sequencing projects have revealed that mutation rates display 10- to 100-fold differences among cancer types and even among different cancers of the same type (18–20). A low mutation rate appears to be a general feature of pediatric cancers (21), challenging the view that genomic instability is critical for tumor progression. A low mutation frequency so far has been observed in medulloblastoma (22), rhabdoid cancers (23), glioblastoma (24), retinoblastoma (25), and seems to be a feature of Ewing sarcoma (20). Hence, the patho-mechanisms of Ewing sarcoma and suitable molecular therapeutic targets have mostly remained elusive. However, even in translocation-driven tumors, multiple clones with varying genetic aberrations and driving capacity for the disease may occur (26). Ewing sarcoma has been reported to contain a low number of mutations in coding regions (20). Given the still dismal prognosis of advanced Ewing sarcoma (27, 28), we performed whole genome sequencing (WGS) of diagnosis and relapse samples to identify potential drivers and relapse-associated genes. Furthermore, we performed exome sequencing to expand the findings and to identify novel therapeutic targets.

Materials and Methods

Patient material

Patient material was obtained from clinical studies of the Cooperative Ewing Sarcoma Study Group (CESS) in Europe. All patients provided informed consent.

Nucleic acid extraction

We extracted nucleic acids from peripheral blood leukocytes, tumor material, and cell cultures by use of either the DNAeasy or the RNAeasy Blood and Tissue Kit (Qiagen) according to the supplier's recommendations.

Whole-genome sequencing

WGS was performed at Complete Genomics using 10 μg of high molecular weight DNA. Sequences were mapped to the National Center for Biotechnology Information (NCBI, Bethesda, MD) reference genome build 37. Unless explicitly stated otherwise, all computations were performed using the statistical environment R (http://www.r-project.org).

Exome sequencing

Exomes were enriched in solution with SureSelect XT Human All Exon 50 Mb kits (Agilent Technologies) and sequenced as 100 bp paired-end runs using TruSeq SBS chemistry v3 (Illumina) generating 5 to 12 Gb of sequence and an average read depth between 66 and 166 on target regions. More than 90% of the target regions were covered 20 times or more. Burrows-Wheeler Aligner (BWA v 0.5.9) with standard parameters was used for read alignment against the human genome

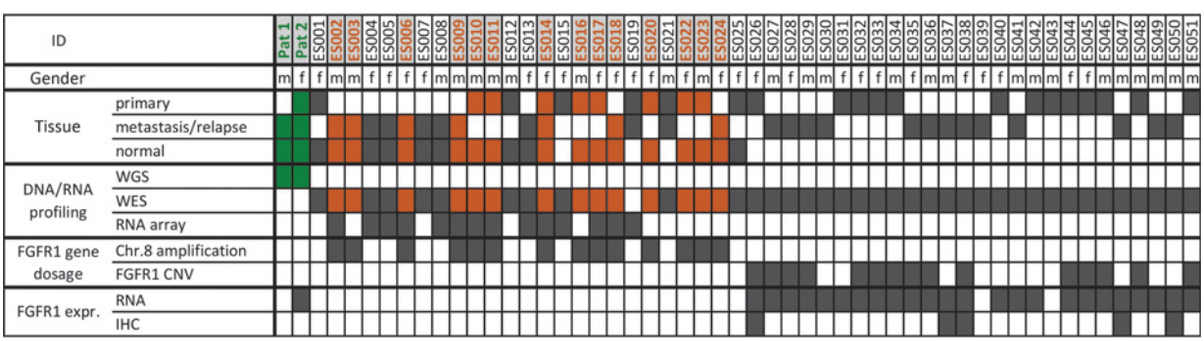

Figure 1.
Combined patient characteristics and subjected methods. For WGS (green) and WES, tumor samples derived from 52 Ewing sarcoma patients were used. A discovery dataset of 14 matched tumor–normal pairs (orange) allowed identification of somatic mutations and analysis of chr8 amplification. *FGFR1* copy number (CNV) was analyzed by real-time PCR. Expression of FGFR1 was determined either on RNA level by microarray technology or real-time PCR or on protein level by immunohistochemistry (IHC). Additional sarcomas were analyzed for FGFR1 expression or CNV only (Supplementary Fig. S1).

Published OnlineFirst July 15, 2015; DOI: 10.1158/1078-0432.CCR-14-2744

assembly hg19 (GRCh37). We performed single-nucleotide variant and small insertion and deletion (indel) calling for the regions targeted by the exome enrichment kit using SAMtools (v 0.1.18). Large indels were called with Pindel (v 0.2.4t) and copy number variations (CNV) were determined using the R package ExomeDepth (v 0.9.7).

To discover putative somatic variants, we retrieved only those variants of a tumor that were not found in the corresponding control tissue. To reduce the number of false positives, we filtered out variants that were already present in 3,600 "in-house" control exomes (patients with unrelated diseases and healthy controls from other projects) or had variant quality of less than 30. Furthermore, the variants were filtered according to several quality criteria using the SAMtools varFilter script. We used default parameters, with the exception of the maximum read depth (−D) and the minimum *P* value for base quality bias (−2), which we set to 9999 and 1E−400, respectively. Moreover, we applied a custom script that marked all variants where the median base quality of adjacent bases was low, because these variants are often sequencing artifacts. We then manually investigated the raw read data of the remaining variants using the Integrative Genomics Viewer (IGV v2.3.19).

FGFR1 copy number

Real-time PCR. *FGFR1* gene copy number was determined using TaqMan copy number assays (Life Technologies) according to the supplier's protocol. In brief, each 10 ng of genomic DNA was used for duplexed real-time PCRs targeting human *FGFR1* and *RNase P* gene. Reactions were carried out in duplicates. Gene copy number was calculated using Copy Caller v2.0 software.

Interphase fluorescent* in situ *hybridization. Cells were grown under standard culture conditions. Standard cytogenetic techniques were used for harvesting, isolation of interphase nuclei, and slide preparation. Fluorescent *in situ* hybridization (FISH) was

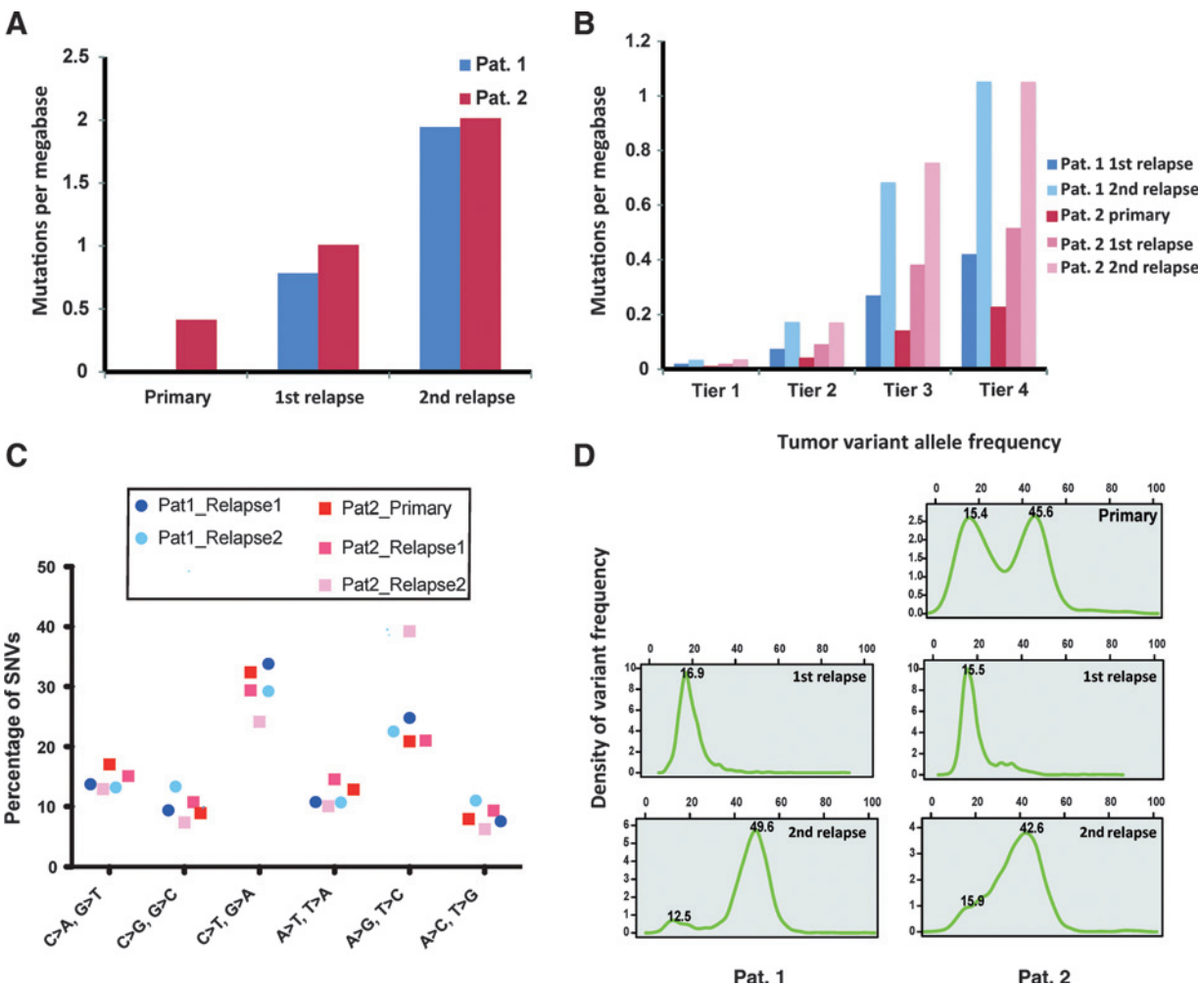

Figure 2.
WGS analysis of Ewing sarcomas. A, frequency of somatic mutations per megabase of genomic DNA in primary and relapsed samples. A 2- to 3-fold increase was shown for each relapse. B, classification of somatic mutations using a tier-4 scheme (tier 1, within coding regions; tier 2, within conserved regions; tier 3, nonrepetitive regions; and tier 4, the remaining ones). C, percentage of the observed mutations within the six different possible base-pair substitutions. D, clonality analysis based on mutant allele frequency in WGS data. Only SNV for sequenced alleles with >50× coverage were used. Allele frequency was not corrected for DNA contribution of non-tumor cells.

Published OnlineFirst July 15, 2015; DOI: 10.1158/1078-0432.CCR-14-2744

carried out using a dual-labeled break-apart probe (Kreatech) targeting *FGFR1* and surrounding sequences of 1.1 MB length and a centromere 8 probe. Nuclei were counterstained with DAPI.

FGFR1 expression

Immunohistochemistry. Slides of the 41 Ewing sarcoma samples were deparaffinized and rehydrated. Primary antibody targeting FGFR1 and horseradish peroxidase (HRP)–coupled secondary antibody was used for antigen detection. Staining intensities were graded semi-quantitatively based on the percentage of positive cells (0: negative, 1: <25%, 2: <50%, 3: >50%) using positive controls recommended by the antibody supplier.

Real-time RT-PCR. Reverse-transcribed mRNA of 61 Ewing sarcoma was used for quantification of FGFR1 expression by means of SYBR green real-time PCR. GAPDH was used as housekeeping gene and FGFR1 expression was calculated relative to the expression in the Ewing sarcoma cell line VH-64 using the $2^{-\Delta CT}$ method.

In vitro studies

FGFR1 knockdown and proliferation. Cells were lentivirally transduced with the vector pLKO-GFP containing two different shRNAs against human FGFR1. Scrambled shRNA sequence cloned into pLKO-GFP served as control. Cells were FACS sorted for GFP expression after 48 hours. For adherent cell lines (A673, SK-NMC,

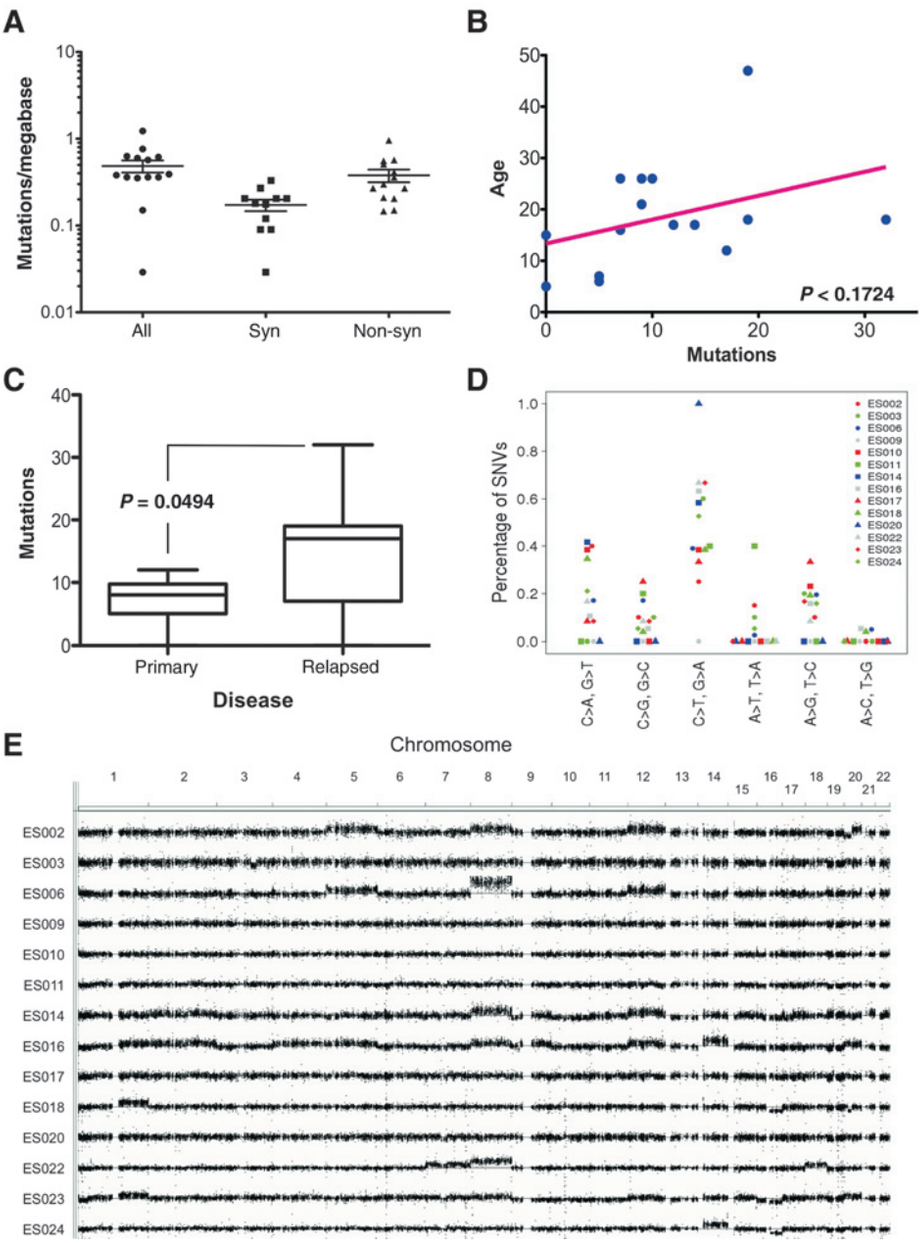

Figure 3.
WES analysis of Ewing sarcoma; analysis of somatic mutations in 14 tumor–normal pairs (7 primary, 6 relapsed, and for 1 both; male:female 1:1; median age at sampling 18.4 years; range, 5–47 years). A, frequency of protein-coding (non-syn) and silent somatic mutations (syn) per megabase of genomic DNA. B, number of observed somatic mutations per age. Each dot represents an individual patient. C, quantity of somatic mutations in newly diagnosed patients (primary) and patient samples with relapsed disease. D, percentage of the observed mutations within the six different possible base-pair substitutions. E, observed CNVs across autosomes in individual tumor–normal pairs of the exome discovery dataset.

Published OnlineFirst July 15, 2015; DOI: 10.1158/1078-0432.CCR-14-2744

and A549), 50,000 cells per well were seeded into 24 wells in a 12-well plate format, whereas 5,000 cells were used for suspension cell lines (KASUMI, HL60). Cells were cultured under standard conditions in RPMI medium containing 10% FCS. Cell numbers were determined every day for 5 consecutive days. Biologic replicates were performed.

FGFR1 mutagenesis and proliferation. FGFR1 cDNA (ThermoFisher CloneID: 3911101) was mutated (N546K) using the QuikChange Lightning Site-Directed Mutagenesis Kit (Agilent Technology) following the suppliers instructions. Wild-type and mutated cDNA was cloned into MSCV2.2-GFP and transduced into NIH-3T3 cells using standard techniques. Effect of N546K on proliferation was analyzed as described above for adherent cell lines.

FGFR1 mutagenesis and colony forming. Soft agar assays were used to determine the effect of N546K on colony-forming capacity. Briefly, 10,000 cells per well were transduced with either control, wild-type, or mutated *FGFR1*. After mixing with agarose and plating, they were allowed to form colonies for 7 days.

Animal model

Immune deficient Rag2$^{-/-}\gamma_C{}^{-/-}$ mice on a BALB/c background were obtained from the Central Institute for Experimental Animals (Kawasaki, Japan) and maintained in our animal facility in Munich under pathogen-free conditions in accordance with the institutional guidelines and approval by local authorities. Experiments were performed in 5 mice per group at the age of 6 to 10 weeks.

In vivo experiments

For the analysis of *in vivo* tumor growth, cells were harvested by trypsinization, washed with Dulbecco's phosphate-buffered saline, and injected in a volume of 0.2 mL into immune deficient Rag2$^{-/-}\gamma_C{}^{-/-}$ mice. To investigate local tumor growth, 2×10^6 Ewing sarcoma cells and derivatives were injected subcutaneously into the groin using a 26-gauge needle attached to a 1 mL syringe. Tumor size was determined as described previously (1). Mice bearing a tumor >10 mm in diameter were considered as positive and sacrificed.

Additional statistical analysis

Descriptive statistics is used to determine parameters like mean, standard deviation, and standard error of the mean (SEM) from more than two independent experiments. Differences were analyzed by an unpaired two-tailed Student *t* test as indicated using Excel (Microsoft) or Prism 5 (GraphPad Software); $P < 0.05$ were considered statistically significant (*, $P < 0.05$; **, $P < 0.005$; ***, $P < 0.0005$).

Results

Specimens from 116 Ewing sarcoma patients were investigated in this project. Matched normal, primary, and relapse specimens from two patients were analyzed by WGS (Fig. 1; green-labeled specimens). For exome sequencing and expression analysis, we used tumor samples of 51 patients (Fig. 1; ES001–ES051). For 24 of these patients, normal tissue controls were available. We performed whole exome sequencing (WES) in a discovery set of 14 of the matched tumor/normal sample pairs that was selected on the basis of average coverage and high tumor content (for seven primary only, for six relapsed only and for one both; Fig. 1, orange-labeled specimens). As a validation cohort, we performed exome sequencing on further 36 Ewing sarcoma patients (17 primary with three matched normal tissues, 18 relapses with five matched normal tissues, and one with primary and relapse) for the detection of recurrent mutations. Expression data were obtained from tumor material from 14 of 53 patients, which were analyzed by WES and compared with a normal body map of 21 different healthy tissues [normal body atlas (NBA) see Supplementary Materials and Methods]. Finally, the remaining 63 of 116 Ewing sarcoma patient samples were used for analysis of FGFR1 DNA copy number gain, mRNA profiling, and immunohistochemistry. Combined patient characteristics and subjected methods are shown in Fig. 1 and Supplementary Fig. S1.

WGS in patients with relapses of Ewing sarcoma

Patient #1 was a 36-year-old male with first diagnosis of Ewing sarcoma in the left tibia. One year after multimodal therapy the patient relapsed locally. A second local relapse occurred along with lung metastases 1 year later. Ultimately, the patient died of the disease 8 months later. WGS was performed using specimens obtained from the first and second relapse and peripheral blood as germline control.

The female patient #2 was 12 years old at diagnosis of the primary tumor in the left pubic bone and the left acetabulum and lung metastases. She was treated according to the EURO-Ewing-99-protocol. The first relapse, lung metastases and local recurrence, occurred 2 years after diagnosis. Three years later, the second pulmonary relapse was diagnosed. Samples for WGS were

Table 1. Genes with significant frequencies of recurrent mutations across 50 Ewing sarcomas (ES)

Name	Gene description	Recurrence	Frequency (%)	*P*[a]	*q* value[a]	Expression (FC)[b]	Comment
ANKRD30A	Ankyrin repeat domain 30A	5	9.6	4.11E−05	1	1.02	Ubiquitious
CCDC19	Coiled-coil domain containing 19	6	11.5	4.39E−04	1	0.92	Ubiquitious
KIAA0319	—	4	7.7	1.20E−02	1	0.57	Increased in fetal brain
KIAA1522	—	4	7.7	1.60E−02	1	0.69	Increased in brain, fetal brain
LAMB4	Laminin, beta 4	5	9.6	3.57E−02	1	1.03	Ubiquitious
SLFN11	Schlafen family member 11	4	7.7	1.60E−02	1	10.91	Increase in ES
STAG2	Stromal antigen 2	6	11.5	4.74E−05	4.47E−01	2.10	Increase in ES, also in cerebellum
TP53	Tumor protein p53	3	5.7	4.46E−04	1	1.79	Increase in ES
UNC80	unc-80 homolog	4	7.7	4.32E−02	1	0.36	Increased in brain
ZNF98	Zinc finger protein 98	4	7.7	1.08E−02	1	1.34	Ubiquitious

[a]Based on the MutSigCV algorithm (http://www.broadinstitute.org/cancer/cga/mutsig).
[b]FC of expression of Ewing sarcoma samples compared with a normal body map (GSE45544).

Published OnlineFirst July 15, 2015; DOI: 10.1158/1078-0432.CCR-14-2744

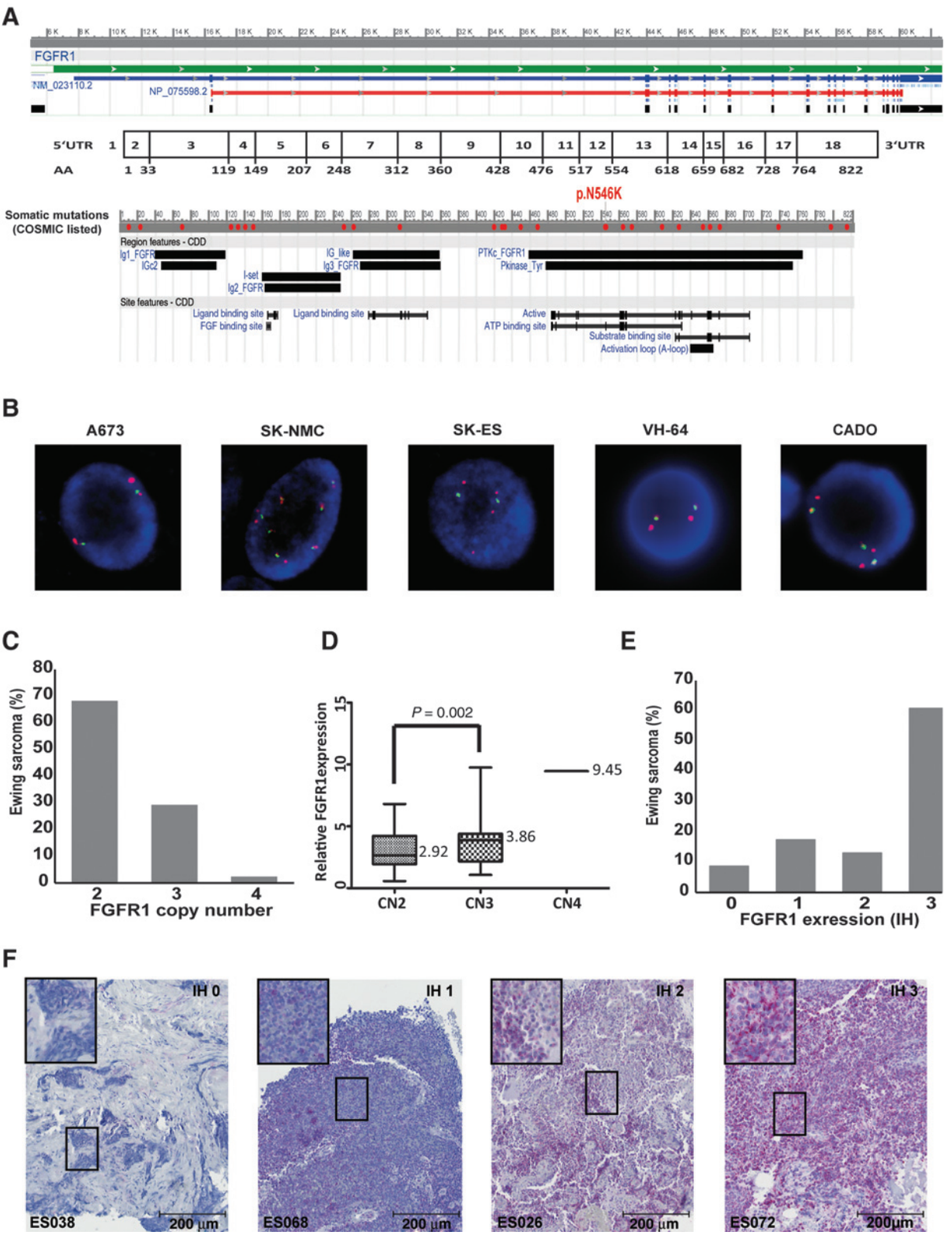

Figure 4.
FGFR1 in Ewing sarcomas. A, structure, functional domains, and known and identified (p.N546K) recurrent somatic mutations of *FGFR1* (figure modified according to NCBI). B, *FGFR1* targeting interphase FISH in cell lines of the Ewing sarcoma family using a *FGFR1* locus-specific break-apart probe spanning 1.1 Mbp (red/green) and a centromere 8 probe (red). C, *FGFR1* copy number in Ewing sarcoma determined by TaqMan-based copy number assays. Duplexed real-time PCRs targeting human *FGFR1* and *RNase P* were performed to calculate copy number using Copy Caller 2 software (Life Technologies). (*Continued on the following page.*)

Published OnlineFirst July 15, 2015; DOI: 10.1158/1078-0432.CCR-14-2744

taken from peripheral blood, the primary tumor, and two consecutive pulmonary relapses.

In both patients, the EWS-FLI1 mutation was present in all diagnostic and relapse samples.

Randomly selected somatic mutations obtained via WGS were verified by Sanger sequencing to develop receiver-operating curves (ROC) that enabled accurate quantitation of mutation load per mega base (Supplementary Table S1 and Supplementary Fig. S2). In the female patient, the total number of somatic mutations was 1,325 and doubled with each relapse (first relapse = 3,229 mutations; second relapse = 6,443 mutations), indicating that recurrent disease appeared to consistently double the number of somatic mutations (Fig. 2A). Similar findings were obtained in the male patient with 2,506 mutations at first sample and 6,219 mutations in the second sample. Interestingly, the 2- to 3-fold increase in mutation rate for each relapse was consistent among different types of mutations. For single-nucleotide variations (SNV), there was a 1.9- to 2.5-fold increase in mutation frequency. Deletions occurred in relapsed samples at a 2.7- to 3.2-fold increase compared with the previous specimen (Supplementary Fig. S2B). These findings suggest that despite different treatments, the increasing genomic instability of Ewing sarcoma is evenly distributed among different mutation types. Nonetheless, deletions occurred up to two times more frequently than insertions. This trend was observed in all direct comparisons of recurrence with previous tumor stage. Between 100 and 500 mutations per specimen affected exonic regions. Of these, only a minority between 27 and 115 were found as tier 1 mutations with expected functional consequences for coding proteins (Fig. 2B). In line, a strong increase was observed from the time of diagnosis to the consecutive relapsed situations (patient #1: first relapse = 61 mutations; second relapse = 109 mutations; patient #2: primary = 27 mutations; first relapse = 62 mutations; second relapse = 115 mutations). The increase in mutation frequency was about 2-fold (Supplementary Fig. S2C). Mutations were evenly distributed throughout the genome in the male patient (Supplementary Fig. S3A, left) as well as in the female patient with primary tumor, first, and second relapse (Supplementary Fig. S3A, right). A further analysis of the mutation types for SNVs revealed that cytosine conversions into thymidine were most frequent followed by adenosine (A) to guanosine (G) transversions (Fig. 2C), which was similarly observed after exome sequencing (Fig. 3D). C to T conversions are frequently observed in damaged long single-strand DNA regions due to the activity of APOBEC enzymes (29, 30). Of note, in the second relapse of the female patient the A to G mutation was most frequently observed.

In the female patient, two major clones were observed at the time of diagnosis (Fig. 2D). At the time of first and second relapse, only one predominant clone was observed with indications for smaller subclones. In the male patient, only one major clone was observed and one predominant clone was present also at the time of second relapse. These findings indicate that clonal heterogeneity does exist in Ewing sarcoma. Also, similar to other cancers, it is likely that clonal selections occur via chemotherapy and are associated with fewer subclones in relapses.

WES of Ewing sarcoma patient samples

In addition to WGS in primary and relapse patients, we sought to further identify the spectrum of mutations in Ewing sarcoma. In a discovery dataset of 14 individual patients (7 primary, 6 relapsed, and 1 patient where both primary and relapse were available), we analyzed matched tumor/normal pairs. High tumor cell content, the availability of matched normal tissue, and the high quality and amount of DNA enabled exome sequencing analysis with especially high sensitivity and specificity. As a validation cohort, we performed exome sequencing of further 36 Ewing sarcoma (17 primary, 18 relapses, and one with both) for the detection of recurrent mutations; part of them (8 samples) matched to normal controls. The Ewing sarcoma samples in the discovery cohort in their majority exhibited EWS/FLI1 translocations (Supplementary Table S2). To reduce the number of false positives, we filtered out variants that were already present in 3,600 "in-house" control exomes (see Materials and Methods). The matched tumor/normal pairs were used to identify the rate of somatic mutations per megabase exomes. We identified 232 somatic mutations in 14 Ewing sarcoma, of which 166 were damaging mutations leading to loss of protein function. On average, 0.38 somatic mutations per megabase were observed in Ewing sarcoma. Most of these mutations were nonsynonymous mutations (Fig. 3A). Pediatric tumors have been reported to harbor a low number of mutations (21), a finding that was recapitulated in our study. However, Ewing sarcoma also occurs in adult patients. Importantly, in our investigation the mutation rate did not increase significantly with age of the patient (Fig. 3B). This indicates that age is not the determining factor for the number of mutations in Ewing sarcoma. Also, higher mutation load and increased genomic instability might not be the reason for the less favorable outcome of Ewing sarcoma in adult patients. Primary tumors harbored on average nine mutations per exome, whereas around 18 mutations per exome were found in relapsed tumors (Fig. 3C). This again is in line with the finding in the WGS that relapses are associated with a 2- to 3-fold increased number of somatic mutations. Examples comprising mutation patterns in particular patients are given in Supplementary Fig. S3B.

For subsequent analysis of mutation frequency, 36 additional Ewing sarcoma samples were investigated by WES. This approach identified a set of recurrently mutated genes. The further examination was performed according to presumed variations in patient-specific mutation frequency and gene-specific background mutations by use of the MutSig algorithm (http://www.broadinstitute.org/cancer/cga/mutsig). The MutSig analysis led to a list of genes with nonsynonymous mutation frequencies ranging from 5.7% to 11.5% (Table 1 and Supplementary Table S4). Mutations in, for example, ankyrin repeat domain-containing protein 30A (*ANKRD30A*; at 9.6%), coiled-coil domain containing protein 19 (*CCDC19*, at 11.5%), laminin, β 4 (*LAMB4*; at

(*Continued*.) D, correlation of FGFR1 copy number and gene expression. Copy number (CN) was determined as explained above and RNA expression by means of SYBR green real-time PCR. GAPDH was used as a housekeeping gene, and FGFR1 expression was calculated relative to the expression in the Ewing sarcoma cell line VH-64 using the $2^{-\Delta CT}$ method. Expression correlated significantly with copy number as calculated with the Wilcoxon signed-rank test (CN2, $n = 16$; CN3, $n = 10$; CN4, $n = 1$). E, FGFR1 expression (0, neg; 1, weak; 2, mod.; 3, strong) in Ewing sarcoma by means of immunohistochemistry (IHC). F, IHC of FGFR1 of representative Ewing sarcoma samples (IHC intensities: ES068 = 0, ES074 = 1, ES026 = 2, ES080 = 3).

Published OnlineFirst July 15, 2015; DOI: 10.1158/1078-0432.CCR-14-2744

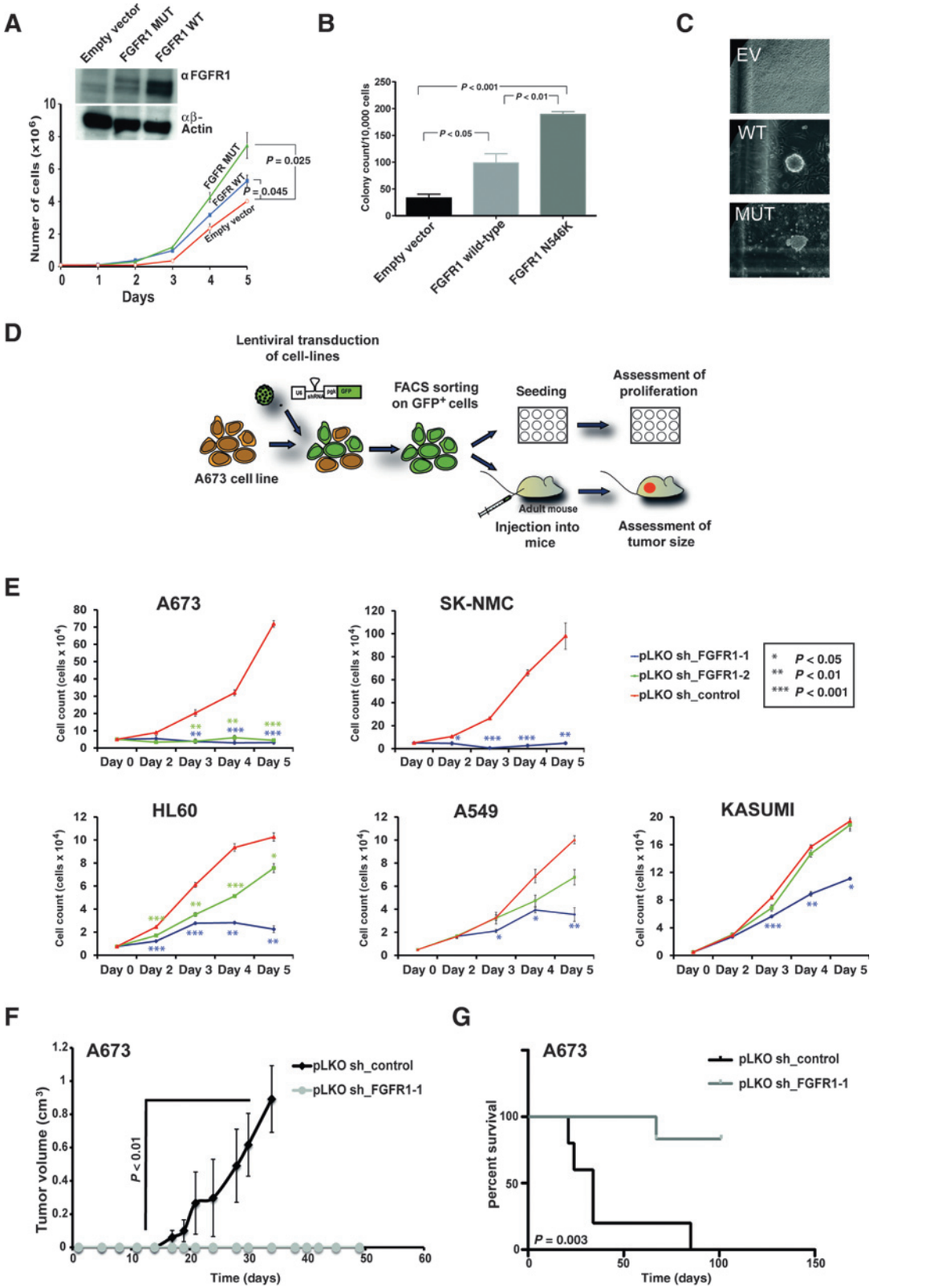

Published OnlineFirst July 15, 2015; DOI: 10.1158/1078-0432.CCR-14-2744

9.6%), schlafen family member 11 (*SLFN11*; at 7.7%), unc-80 homolog (*UNC80*; at 7.7%), and zinc finger protein 98 (*ZNF98*; at 7.7%) may involve different aspects of tumor pathology presumably important but not essential for disease development.

However, such recurrent mutation as filtered by the MutSig algorithm where of low statistical significance (with no FDR value below 0.1; Table 1). Silencing mutations of stromal antigen 2 (*STAG2*) in Ewing sarcoma were recently described (31–34) and were confirmed by Sanger sequencing (Supplementary Fig. S4A). The presumed aneuploidy in cases with *STAG2* mutations as described by others (31) was not confirmed in our study similar to other published observations (35).

Comparison with expression data interestingly demonstrated an upregulation of SLFN11 [fold change (FC) = 10.9], STAG2 (FC = 2.1), and TP53 (FC = 1.79) in Ewing sarcoma when compared with the mean of a normal body map of healthy tissue (NBA; see Supplementary Materials and Methods; Table 1 and Supplementary Tables S4 and S5). Others, like ANKRD30A, CCDC19, LAMB4, or ZNF98, were ubiquitously expressed, whereas some were up in brain or fetal brain tissue, such as KIAA0319, KIAA1522, or UNC80, which is also true for STAG2.

Furthermore, analysis of overlapping somatic mutations in three different patient triplets of primary and relapsed tumor samples (Pat. 1 and 2, and ES014) revealed recurrent mutations for each patient (Supplementary Table S5). Overall, a large amount of mutations were shared in consecutive sarcomas (Pat. 1: 61 mutations in relapse 1, of these 42 shared with relapse 2; Pat. 2: 27 mutations in primary, of these 8 shared with relapse 1 and/or relapse 2; ES014: 13 mutations in primary, of these 9 shared with metastasis).

Overall, the observed low frequency of recurrent nonsynonymous mutations of which only *STAG2* seemed to be statistically significant suggests that collaborative events in Ewing sarcoma do not require SNV in addition to EWS/ETS translocations.

Deregulation of FGFR-1 in Ewing sarcoma

Exome sequencing was performed to identify novel driver genes in Ewing sarcoma. Interestingly, one somatic mutation in the male patient with Ewing sarcoma that underwent WGS was a known oncogenic mutation in *FGFR1*. This mutation (N546K) occurred in the tyrosine kinase domain (Fig. 4A) and was independently discovered as an activating mutation in pilocytic astrocytoma and glioblastoma (36, 37). This mutation was confirmed in all tumor specimens from this patient (Supplementary Fig. S4B). Sanger sequencing of the *FGFR1* kinase domain in 30 additional Ewing sarcoma specimens did not reveal additional mutations (data not shown). As a complementary approach for the identification of driver events, we used exome data to identify CNVs. Deletions involving different exons of cyclin-dependent kinase inhibitor 2a (*CDKN2A*; ref. 15) were observed in four of 14 tumors, but gain of chromosome 8, which was found in five of the 14 tumors, was among the most frequent alterations (Fig. 3E). This is in line with previous findings (15, 38). Trisomy 8 and amplifications of chromosome 8 are the most frequent cytogenetic findings in Ewing sarcoma (14). The relevant gene or the relevant genes have not been identified so far. Of note, all amplifications involve the *FGFR1* gene.

FGFR1 is located on chromosome 8p, and we next analyzed the copy number status of *FGFR1* in Ewing sarcoma. A real-time PCR–based method identified a gain of the *FGFR1* locus in 13 of 41 patients (31.7%). Of these, 12 patients had gained one copy and one patient harbored four gene copies (Fig. 4C). Our analyses included copy number gains due to chr8 amplification as well as direct gene copy number gain. *FGFR1* copy numbers closely correlated with FGFR1 gene expression (Fig. 4D). Gains of *FGFR1* copy number did not only occur in primary tumors, but were consistently observed in Ewing sarcoma cell lines A673, CADO, SK-NMC, SK-ES, and VH-64. Copy number gains of *FGFR1* occur due to trisomy 8 in the majority of patients but a proportion of patients and cell lines also showed amplification beyond three copies of the entire chromosome (Fig. 4B).

In line, FGFR1 was highly expressed in Ewing sarcoma on the mRNA level (Supplementary Fig. S5A and S5B) and on the protein level as indicated by immunohistochemistry (Fig. 4E and F).

Functional analyses of FGFR1 expression in Ewing sarcoma

Activating mutations, copy number gains and other alterations as well as increased expression of FGFR1 occur in Ewing sarcoma (e.g., compared with normal tissue; Supplementary Fig. S5B) with a high frequency. We therefore further analyzed the potential role of FGFR1 in Ewing sarcoma. First, we retrovirally transduced FGFR1 wild-type or the FGFR1 N546K mutant into NIH3T3 cells. Both, overexpressed FGFR1 wild-type and the N546K mutation enhanced proliferation (Fig. 5A). In colony formation assays, FGFR1 N546K mutation more than quadrupled the number of colonies obtained after empty vector transduction, whereas the FGFR1 wild-type doubled colony formation (Fig. 5B). The transformation of NIH3T3 cells by FGFR1 wild-type and FGFR1 N546K mutation is also indicated in Fig. 5C by the formation of three-dimensional clusters. Alterations of FGFR1, especially the gain of the locus as well as expression of the protein, were associated with a trend toward inferior survival in patients with Ewing sarcoma (Supplementary Fig. S6).

To analyze whether FGFR1 signaling was required for Ewing sarcoma growth, we performed shRNA-based knockdown after transduction with lentiviral constructs encoding scrambled (pLKO_shcontrol) or FGFR1-specific shRNA (pLKO_shFGFR1), respectively. Specific shRNA knockdown suppressed FGFR1 mRNA expression by 70% or more in Ewing sarcoma cell lines and was confirmed on the protein level too (Supplementary

Figure 5.

Functional analyses of FGFR1. A, proliferation of NIH-3T3 cells expressing a control (empty vector), wild-type (WT), or mutant (MUT) FGFR1. B, colony-forming capacity of NIH-3T3 cells according to wild-type and mutant FGFR1 expression. C, representative colonies of NIH-3T3 cells expressing a control (EV), wild-type (WT), or mutant (MUT) FGFR1. Only FGFR1-expressing cells (WT and MUT) showed three-dimensional clusters indicating cellular transformation. D, diagram of the generation of A673 FGFR1 knockdown cells by lentiviral transduction and their use for *in vitro* and *in vivo* analyses. E, proliferation of cell lines after lentiviral infection with scrambled (pLKO_shcontrol) or FGFR1-specific shRNA constructs (pLKO_shFGFR1; Ewing sarcoma family: A673 and SK-NMC; leukemia: HL60 and KASUMI, lung carcinoma: A549). F, mice were injected with A673 cells infected with scrambled shRNA (pLKO_shcontrol) or FGFR1 shRNA (pLKO_shFGFR1). Tumor growth until day 50 is shown. G, survival curve of $Rag2^{-/-}\gamma c^{-/-}$ mice after s.c. injection of A673 FGFR1 shRNA (pLKO_shFGFR1) and scrambled shRNA-transduced (pLKO_shcontrol) cells, respectively as shown in F. Only 1 mouse of the group of mice injected with A673 FGFR1 shRNA infectants (pLKO_shFGFR1) developed a tumor at day 67 after inoculation.

Published OnlineFirst July 15, 2015; DOI: 10.1158/1078-0432.CCR-14-2744

Fig. S5C and S5D). Knockdown of FGFR1 inhibited growth of Ewing sarcoma and other cancer cells such as the A549 lung carcinoma cell line or the leukemia cell lines HL60 and Kasumi. Of note, almost complete growth suppression was observed only in the Ewing sarcoma cell lines (Fig. 5D).

To analyze whether FGFR1 inhibition was also relevant for Ewing sarcoma growth *in vivo*, lentivirally transduced A673 Ewing sarcoma cells were injected into $Rag2^{-/-}\gamma_C^{-/-}$ mice (6). Viability at the time of injection was 100% for both scrambled (pLKO_sh-control) and FGFR1 shRNA (pLKO_shFGFR1) transduced cell lines. However, mainly scrambled transduced A673 cells formed tumors in mice (100%), whereas only in 1 mouse a tumor was formed by FGFR1 shRNA (pLKO_shFGFR1) transduced cells. Tumor growth and survival curves are shown in Fig. 5F and G. These findings suggested that FGFR1 is a crucial signaling pathway for Ewing sarcoma.

Ponatinib is a tyrosine kinase inhibitor (TKI) that among others, effectively targets FGFR1 at low nanomolar concentrations (39). Accordingly, proliferation of all tested Ewing sarcoma cell lines was inhibited by ponatinib treatment in the nanomolar range of concentrations (Supplementary Fig. S6C). One patient with Ewing sarcoma, who had exhausted all other treatment options, was offered ponatinib treatment. FGFR1 inhibition by ponatinib elicited a response by significantly decreasing the glucose uptake of the tumor (Supplementary Fig. S6D). The treatment effect was not maintained and the patient eventually died with clinical progress of CNS metastases (brain and meninges).

Discussion

Pediatric malignancies, and especially Ewing sarcoma, have been reported to contain few if any recurrent mutations (21, 33, 34). Our study leads to important novel insights into the pathogenesis of Ewing sarcoma. First, the mutation load in Ewing sarcoma remains very low on WGS as well as WES level. No frequent genetic driver mutation besides the well-described *EWS/ETS* translocation was identified (40). Mutation load did not depend on age at diagnosis that suggests that mutation load does not play an important factor for the worse prognosis observed in adult patients. It appears that the number of observed mutations in Ewing sarcoma is disease specific and was not closely associated with patient age at the time of diagnosis. This is in contrast to age-associated cancers such as AML, which show increased mutation load in older patients (41). Despite the unifying events of the balanced *EWS/FLI1* translocation, clonal subpopulations exist. These contain different mutations, which are only partially overlapping. Signs of clonal selection are present in relapse specimens and each relapse was associated with a 2- to 3-fold increase in somatic mutation load compared with the primary tumor or the previous relapse. So far, no targetable mutations had been reported in Ewing sarcoma. In our study, we identified alterations of the *FGFR1* gene as a highly frequent event in Ewing sarcoma pathogenesis. We initially discovered a somatic point mutation in the tyrosine kinase domain with activating activity in two subsequent relapse specimen indicating stability of the mutation. The structural analysis of this mutation (37) as well as functional analyses provide evidence that this N546K mutation induces enhanced FGFR1 activity and increased proliferation. In addition, wild-type FGFR1 is overexpressed in many Ewing sarcoma tumors. Forced expression of FGFR1 increased proliferation and clonogenic growth in fibroblasts. Intriguingly, copy number gain of *FGFR1* was detected in a substantial fraction of Ewing sarcoma either due to gene amplification or Trisomy 8 cytogenetic aberration. Trisomy 8 is the most frequent cytogenetic aberration that is found in Ewing sarcoma but no involvement of a specific gene locus was identified so far (14, 38). Accordingly, FGFR1 was highly expressed on the protein level in almost all analyzed Ewing sarcoma. Gene amplification and overexpression are crucial pathogenetic mechanisms for growth factor receptors activation in multiple cancers (42, 43). For example, *EGFR* amplification and overexpression with subsequent auto-activation has been described in breast cancer and lung cancer. Along the same line, *Her2/NEU/ERBB2* amplification and expression is of pathogenetic relevance in breast cancer and associated with a poor prognosis (44). The potential relevance of FGFR1 for Ewing sarcoma was suggested in our data by the association of high FGFR1 expression levels with increased relapse rates and more importantly by the fact that suppression of FGFR1 abolished the growth of Ewing sarcoma cell lines. This phenomenon was evident for all analyzed Ewing sarcoma cell lines and was observed *in vitro* as well as *in vivo*. The efficacy of shRNA-based FGFR1 knockdown was far more prominent in Ewing sarcoma than in several other cancer types, such as lung cancer, which had previously been described to be associated with FGFR1 activity (42). Ponatinib as a FGFR1 inhibitor (39) showed significant activity toward proliferation of Ewing sarcoma cell lines in our experiments. Of note, proliferation of all Ewing sarcoma cell lines was inhibited by ponatinib (Supplementary Fig. 6C).

Ewing sarcoma cells appear to be far more addicted to FGFR1 signaling than carcinoma cells that implies that FGFR1 inhibitors should be tested in Ewing sarcoma. In addition to the preclinical data for ponatinib, we also treated 1 patient with Ewing sarcoma, who had exhausted all available therapy options, with ponatinib monotherapy. Tumor activity was assessed by positron emission tomography scanning. After 3 weeks of therapy, 18F-FDG-glucose uptake was widely reduced. This may be due to FGFR1 inhibition, but we do not rule out at all that other tyrosine kinases may be involved. Taken together, these data suggest that FGFR1 might be a suitable therapeutic target in Ewing sarcoma. Two main conclusions that can be drawn from our data concern the role of tyrosine kinase alterations in Ewing sarcoma and the approaches to identify driver mutations in cancers with a low frequency of recurrent mutations. Mutations that are not found to be recurrent in a significant fraction of cancers are usually considered to be bystander or passenger mutations. In many studies, these mutations are neglected, but the direct association between nonrecurrent and nonfunctional, for example, as passenger mutation, might be misleading. An important role for FGFR1 in Ewing sarcoma pathogenesis is evident not only by the oncogenic point mutation but also by gene copy gain and knockdown studies. Thus, DNA sequencing alone is obviously not sufficient to assign relevant mutations and driver events due to the low frequency of these events in Ewing sarcoma. In contrast, the combination of protein expression, genomics, and functional analysis provided evidence for the involvement of FGFR1 in Ewing sarcoma pathogenesis. Given the high frequency of trisomy 8, it can be envisioned that about half of all Ewing sarcoma patients show copy number gain of FGFR1 on the genetic level. Increased protein expression that might be even more widespread can also be influenced and induced by multiple other mechanisms, many of these obviously need to be defined for future studies.

Published OnlineFirst July 15, 2015; DOI: 10.1158/1078-0432.CCR-14-2744

Cancers with balanced translocations provide a unique opportunity to identify cooperating events. In some leukemias, a two hit model was proposed that depends on a balanced translocation predominantly affecting self-renewal and differentiation (45). An increased tyrosine kinase activity is a cooperating event that was thought to be responsible preferentially for increased proliferative and antiapoptotic activity. It is obvious that this kind of model is overly simplistic for Ewing sarcoma and FGFR1 alterations are just one event that cooperates with *EWS/ETS* translocations.

In summary, our data provide evidence that integration of genomic data with gene copy number gain, expression, and functional analysis are crucial to identify oncogenic drivers in cancers with low rates of recurrent mutations. FGFR1 may constitute a novel target for therapeutic approaches in Ewing sarcoma.

Disclosure of Potential Conflicts of Interest

E. Wardelmann reports receiving speakers bureau honoraria from Novartis and Pharma Mar, and is a consultant/advisory board member for New Oncology. S. Burdach holds ownership interest (including patents) in PDL Biopharma. No potential conflicts of interest were disclosed by the other authors.

Authors' Contributions

Conception and design: K. Agelopoulos, G.H.S. Richter, U. Dirksen, C. Rossig, D. Baumhoer, S. Burdach, W.E. Berdel, C. Müller-Tidow

Development of methodology: G.H.S. Richter, B. Moser, M. Weckesser, C. Müller-Tidow

Acquisition of data (provided animals, acquired and managed patients, provided facilities, etc.): K. Agelopoulos, G.H.S. Richter, E. Schmidt, U. Dirksen, K. von Heyking, U. Kontny, T. Buch, M. Weckesser, I. Schulze, R. Besoke, A. Witten, M. Stoll, G. Köhler, W. Hartmann, E. Wardelmann, D. Baumhoer, H. Jürgens, S. Burdach, W.E. Berdel, C. Müller-Tidow

Analysis and interpretation of data (e.g., statistical analysis, biostatistics, computational analysis): K. Agelopoulos, G.H.S. Richter, E. Schmidt, B. Moser, H.-U. Klein, M. Dugas, K. Poos, E. Korsching, T. Buch, M. Weckesser, I. Schulze, R. Besoke, C. Rossig, W.E. Berdel, C. Müller-Tidow

Writing, review, and/or revision of the manuscript: K. Agelopoulos, G.H.S. Richter, U. Dirksen, U. Kontny, M. Dugas, K. Poos, E. Korsching, T. Buch, M. Weckesser, I. Schulze, R. Besoke, W. Hartmann, E. Wardelmann, C. Rossig, D. Baumhoer, H. Jürgens, S. Burdach, W.E. Berdel, C. Müller-Tidow

Administrative, technical, or material support (i.e., reporting or organizing data, constructing databases): G.H.S. Richter, U. Dirksen, B. Moser, E. Wardelmann, W.E. Berdel, C. Müller-Tidow

Study supervision: G.H.S. Richter, U. Dirksen, H. Jürgens, C. Müller-Tidow

Acknowledgments

Exome sequencing was performed with help of Tim M. Strom and Thomas Schwarzmayr from the Institute of Human Genetics, Helmholtz-Zentrum München (Neuherberg, Germany). The authors thank Julia Humberg for assistance in sequencing and functional studies and to all C. Müller-Tidow laboratory members for constant help and discussions. The authors are grateful to the team of the CESS group of the Society for Pediatric Oncology and Hematology for the correlation of our findings with the clinical data.

Grant Support

This work is part of the Translational Sarcoma Research Network (TransSaRNet; 01GM0869; 01GM1104B), "Rare Diseases" and Prospective Validation of Biomarkers in Ewing Sarcoma for Personalised Translational Medicine (PROVABES; 01KT1311), Funding Programs of the Federal Ministry of Education and Research (BMBF), Germany. This work was supported by the German Cancer Consortium (DKTK) with help of the German Cancer Research Center (DKFZ), Heidelberg, Germany, and grants from the Else-Kröner-Fresenius Stiftung (2013_A49), the Wilhelm-Sander Stiftung (2009.901.2), and by the Deutsche Forschungsgemeinschaft, DFG (MU 1328/9-1, MU 1328/9-2, and MU 1328-14-1) and EXC 1003 Cells in Motion—Cluster of Excellence, Münster, Germany and the Deutsche Krebshilfe (DKH-108128).

The costs of publication of this article were defrayed in part by the payment of page charges. This article must therefore be hereby marked *advertisement* in accordance with 18 U.S.C. Section 1734 solely to indicate this fact.

Received October 23, 2014; revised May 22, 2015; accepted June 7, 2015; published OnlineFirst July 15, 2015.

References

1. Richter GH, Plehm S, Fasan A, Rossler S, Unland R, Bennani-Baiti IM, et al. EZH2 is a mediator of EWS/FLI1 driven tumor growth and metastasis blocking endothelial and neuro-ectodermal differentiation. Proc Natl Acad Sci U S A 2009;106:5324–9.
2. von Levetzow C, Jiang X, Gwye Y, von Levetzow G, Hung L, Cooper A, et al. Modeling initiation of Ewing sarcoma in human neural crest cells. PLoS One 2011;6:e19305.
3. Ewing J. Diffuse endothelioma of bone. Proc N Y Path Soc 1921;7:17–24.
4. Schmidt D, Harms D, Burdach S. Malignant peripheral neuroectodermal tumours of childhood and adolescence. Virchows Arch A Pathol Anat Histopathol 1985;406:351–65.
5. Staege MS, Hutter C, Neumann I, Foja S, Hattenhorst UE, Hansen G, et al. DNA microarrays reveal relationship of Ewing family tumors to both endothelial and fetal neural crest-derived cells and define novel targets. Cancer Res 2004;64:8213–21.
6. Hauer K, Calzada-Wack J, Steiger K, Grunewald TG, Baumhoer D, Plehm S, et al. DKK2 mediates osteolysis, invasiveness, and metastatic spread in Ewing sarcoma. Cancer Res 2013;73:967–77.
7. Tanaka M, Yamazaki Y, Kanno Y, Igarashi K, Aisaki K, Kanno J, et al. Ewing's sarcoma precursors are highly enriched in embryonic osteochondrogenic progenitors. J Clin Invest 2014;124:3061–74.
8. Aurias A, Rimbaut C, Buffe D, Zucker JM, Mazabraud A. Translocation involving chromosome 22 in Ewing's sarcoma. A cytogenetic study of four fresh tumors. Cancer Genet Cytogenet 1984;12:21–5.
9. Turc-Carel C, Philip I, Berger MP, Philip T, Lenoir GM. Chromosome study of Ewing's sarcoma (ES) cell lines. Consistency of a reciprocal translocation t(11;22)(q24;q12). Cancer Genet Cytogenet 1984;12:1–19.
10. Whang-Peng J, Triche TJ, Knutsen T, Miser J, Douglass EC, Israel MA. Chromosome translocation in peripheral neuroepithelioma. N Engl J Med 1984;311:584–5.
11. Delattre O, Zucman J, Plougastel B, Desmaze C, Melot T, Peter M, et al. Gene fusion with an ETS DNA-binding domain caused by chromosome translocation in human tumours. Nature 1992;359:162–5.
12. Lessnick SL, Ladanyi M. Molecular pathogenesis of Ewing sarcoma: new therapeutic and transcriptional targets. Annu Rev Pathol 2012;7:145–59.
13. Huang HY, Illei PB, Zhao Z, Mazumdar M, Huvos AG, Healey JH, et al. Ewing sarcomas with p53 mutation or p16/p14ARF homozygous deletion: a highly lethal subset associated with poor chemoresponse. J Clin Oncol 2005;23:548–58.
14. Jahromi MS, Jones KB, Schiffman JD. Copy number alterations and methylation in Ewing's Sarcoma. Sarcoma 2011;2011:362173.
15. Mackintosh C, Ordonez JL, Garcia-Dominguez DJ, Sevillano V, Llombart-Bosch A, Szuhai K, et al. 1q gain and CDT2 overexpression underlie an aggressive and highly proliferative form of Ewing sarcoma. Oncogene 2012;31:1287–98.
16. Postel-Vinay S, Veron AS, Tirode F, Pierron G, Reynaud S, Kovar H, et al. Common variants near TARDBP and EGR2 are associated with susceptibility to Ewing sarcoma. Nat Genet 2012;44:323–7.
17. Hanahan D, Weinberg RA. Hallmarks of cancer: the next generation. Cell 2011;144:646–74.
18. Cancer Genome Atlas Research N. Comprehensive genomic characterization defines human glioblastoma genes and core pathways. Nature 2008;455:1061–8.
19. Cancer Genome Atlas Research N. Integrated genomic analyses of ovarian carcinoma. Nature 2011;474:609–15.

Published OnlineFirst July 15, 2015; DOI: 10.1158/1078-0432.CCR-14-2744

20. Lawrence MS, Stojanov P, Polak P, Kryukov GV, Cibulskis K, Sivachenko A, et al. Mutational heterogeneity in cancer and the search for new cancer-associated genes. Nature 2013;499:214–8.
21. Vogelstein B, Papadopoulos N, Velculescu VE, Zhou S, Diaz LA Jr, Kinzler KW. Cancer genome landscapes. Science 2013;339:1546–58.
22. Parsons DW, Li M, Zhang X, Jones S, Leary RJ, Lin JC, et al. The genetic landscape of the childhood cancer medulloblastoma. Science 2011;331:435–9.
23. Lee RS, Stewart C, Carter SL, Ambrogio L, Cibulskis K, Sougnez C, et al. A remarkably simple genome underlies highly malignant pediatric rhabdoid cancers. J Clin Invest 2012;122:2983–8.
24. Wu G, Broniscer A, McEachron TA, Lu C, Paugh BS, Becksfort J, et al. Somatic histone H3 alterations in pediatric diffuse intrinsic pontine gliomas and non-brainstem glioblastomas. Nat Genet 2012;44:251–3.
25. Zhang J, Benavente CA, McEvoy J, Flores-Otero J, Ding L, Chen X, et al. A novel retinoblastoma therapy from genomic and epigenetic analyses. Nature 2012;481:329–34.
26. Greaves M, Maley CC. Clonal evolution in cancer. Nature 2012;481:306–13.
27. Stahl M, Ranft A, Paulussen M, Bolling T, Vieth V, Bielack S, et al. Risk of recurrence and survival after relapse in patients with Ewing sarcoma. Pediatr Blood Cancer 2011;57:549–53.
28. Rasper M, Jabar S, Ranft A, Jurgens H, Amler S, Dirksen U. The value of high-dose chemotherapy in patients with first relapsed Ewing sarcoma. Pediatr Blood Cancer 2014;61:1382–6.
29. Nik-Zainal S, Alexandrov LB, Wedge DC, Van Loo P, Greenman CD, Raine K, et al. Mutational processes molding the genomes of 21 breast cancers. Cell 2012;149:979–93.
30. Roberts SA, Sterling J, Thompson C, Harris S, Mav D, Shah R, et al. Clustered mutations in yeast and in human cancers can arise from damaged long single-strand DNA regions. Mol Cell 2012;46:424–35.
31. Solomon DA, Kim T, Diaz-Martinez LA, Fair J, Elkahloun AG, Harris BT, et al. Mutational inactivation of STAG2 causes aneuploidy in human cancer. Science 2011;333:1039–43.
32. Brohl AS, Solomon DA, Chang W, Wang J, Song Y, Sindiri S, et al. The genomic landscape of the Ewing Sarcoma family of tumors reveals recurrent STAG2 mutation. PLoS Genet 2014;10:e1004475.
33. Crompton BD, Stewart C, Taylor-Weiner A, Alexe G, Kurek KC, Calicchio ML, et al. The genomic landscape of pediatric Ewing Sarcoma. Cancer Discov 2014;4:1326–41.
34. Tirode F, Surdez D, Ma X, Parker M, Le Deley MC, Bahrami A, et al. Genomic landscape of Ewing sarcoma defines an aggressive subtype with co-association of STAG2 and TP53 mutations. Cancer Discov 2014;4:1342–53.
35. Balbas-Martinez C, Sagrera A, Carrillo-de-Santa-Pau E, Earl J, Marquez M, Vazquez M, et al. Recurrent inactivation of STAG2 in bladder cancer is not associated with aneuploidy. Nat Genet 2013;45:1464–9.
36. Jones DT, Hutter B, Jager N, Korshunov A, Kool M, Warnatz HJ, et al. Recurrent somatic alterations of FGFR1 and NTRK2 in pilocytic astrocytoma. Nat Genet 2013;45:927–32.
37. Lew ED, Furdui CM, Anderson KS, Schlessinger J. The precise sequence of FGF receptor autophosphorylation is kinetically driven and is disrupted by oncogenic mutations. Sci Signal 2009;2:ra6.
38. Lynn M, Wang Y, Slater J, Shah N, Conroy J, Ennis S, et al. High-resolution genome-wide copy-number analyses identify localized copy-number alterations in Ewing sarcoma. Diagn Mol Pathol 2013;22:76–84.
39. Gozgit JM, Wong MJ, Moran L, Wardwell S, Mohemmad QK, Narasimhan NI, et al. Ponatinib (AP24534), a multitargeted pan-FGFR inhibitor with activity in multiple FGFR-amplified or mutated cancer models. Mol Cancer Ther 2012;11:690–9.
40. Kovar H. Blocking the road, stopping the engine or killing the driver? Advances in targeting EWS/FLI-1 fusion in Ewing sarcoma as novel therapy. Expert Opin Ther Targets 2014;18:1315–28.
41. Welch JS, Ley TJ, Link DC, Miller CA, Larson DE, Koboldt DC, et al. The origin and evolution of mutations in acute myeloid leukemia. Cell 2012;150:264–78.
42. Wynes MW, Hinz TK, Gao D, Martini M, Marek LA, Ware KE, et al. FGFR1 mRNA and protein expression, not gene copy number, predict FGFR TKI sensitivity across all lung cancer histologies. Clin Cancer Res 2014;20:3299–309.
43. Malchers F, Dietlein F, Schottle J, Lu X, Nogova L, Albus K, et al. Cell-autonomous and non-cell-autonomous mechanisms of transformation by amplified FGFR1 in lung cancer. Cancer Discov 2014;4:246–57.
44. Yan M, Parker BA, Schwab R, Kurzrock R. HER2 aberrations in cancer: implications for therapy. Cancer Treat Rev 2014;40:770–80.
45. Greenblatt SM, Nimer SD. Chromatin modifiers and the promise of epigenetic therapy in acute leukemia. Leukemia 2014;28:1396–406.

Published OnlineFirst July 15, 2015; DOI: 10.1158/1078-0432.CCR-14-2744

Clinical Cancer Research

Deep Sequencing in Conjunction with Expression and Functional Analyses Reveals Activation of FGFR1 in Ewing Sarcoma

Konstantin Agelopoulos, Günther H.S. Richter, Eva Schmidt, et al.

Clin Cancer Res 2015;21:4935-4946. Published OnlineFirst July 15, 2015.